Available online at www.sciencedirect.com
ScienceDirect
Applied Catalysis B: Environmental 79 (2008) 142–148
APPLIED CATALYSIS B: ENVIRONMENTAL
www.elsevier.com/locate/apcatb

The states of gold species in CeO_2 supported gold catalyst for formaldehyde oxidation

Yuenian Shen [a], Xuzhuang Yang [a], Yizheng Wang [a], Yanbing Zhang [a], Huaiyong Zhu [b,*], Ling Gao [c], Meilin Jia [d]

[a] College of Chemistry and Chemical Engineering, Inner Mongolia University, Huhhot 010021, PR China
[b] School of Physical and Chemical Sciences, Queensland University of Technology, Brisbane, QLD 4001, Australia
[c] State Key Laboratory for Oxo synthesis and Selective Oxidation, Lanzhou Institute of Chemical Physics, CAS, Lanzhou 730000, PR China
[d] College of Chemistry, Inner Mongolia Normal University, Huhhot 010022, PR China

Received 3 November 2006; received in revised form 4 September 2007; accepted 24 September 2007
Available online 5 October 2007

Abstract

To develop HCHO oxidation catalysts which work at moderate temperatures, a series of Au/CeO_2 catalysts with a gold content below 0.85 wt.% were prepared by co-precipitation and subsequent calcinations at 300 °C. Oxidation of formaldehyde on these catalysts at temperatures close to 100 °C was conducted, and the structures of catalysts were characterized by X-ray diffraction (XRD) and transmission electronic microscopy (TEM) techniques. Gold exists in highly dispersed crystallite clusters in these catalysts, and we did not observe any gold crystals larger than 2–3 nm. In contrast, the CeO_2 support is well crystallized, the fringes from (1 1 1) lattice plane of the support CeO_2 are very clear in the TEM image. Gold crystals with a mean size of about 10 nm formed in a sample containing 0.78 wt.% of gold (0.78Au) when it was calcinated at 400 °C for 2 h. However, the formation of larger gold crystals causes a decrease in the catalytic activity. It appears that the highly dispersed gold catalyst provides more active sites for the HCHO oxidation. When the sample 0.78Au was calcined at 700 °C for 2 h, large gold particles (≥50 nm) appeared and the activity for HCHO oxidation decreased further but was still better than that of ceria. XRD and XPS results show an interesting fact that some of gold was incorporated into lattice of ceria.

Keywords: Gold catalyst; Formaldehyde oxidation; Indoor air pollution; Ceria support; TEM analysis

1. Introduction

Harmful substances such as benzenoid and aldehyde emitted from the decorating materials could gradually endanger our health. For instance, formaldehyde is widely used in various adhesives and coatings. It is difficult to be completely removed and may emit from house decoration and furniture at an unsafe level for years. Long exposure to the indoor air with a formaldehyde content that is greater than the safe limit can cause serious health problems, such as watery eyes, skin irritation, respiratory diseases, even nasopharyngeal or nasal cancers, etc. [1–4]. The formaldehyde concentration in indoor air of civil residences, schools, hospitals and workshops is strictly regulated. For instance, it has to be below 0.08 mg/m^3 in China [3].

An effective approach for eliminating HCHO of a very low concentration from the indoor air is catalytic combustion which yields CO_2 and H_2O, as final products. The success of this approach greatly relies on the properties of the oxidation catalyst. The desired catalyst should be able to work at lower temperatures and in atmosphere where moisture exists. Moreover, the products of the reaction are H_2O and CO_2 only, and no other by-products should be released. Noble metal catalysts, like platinum, exhibit superior activity for the oxidation of VOCs [5], but their high costs and lack of resources impede their applications. On the other hand, the catalysts of transition metal oxides such as Fe_2O_3, MnO_2, NiO, Co_3O_4 [6] or binary oxides with a rare earth element, such as $LaMnO_3$, $LaFeO_3$, etc. [7,8], exhibit useful catalytic activity only at relative high temperatures. In 1989, Haruta et al. found that gold dispersed on transition metal oxides exhibits high activity for CO oxidation below 0 °C [9] or even at −70 °C [10]. They also reported the catalytic combustion of methanol and its

* Corresponding author. Tel.: +61 7 31381581; fax: +61 7 3864 1804.
E-mail address: hy.zhu@qut.edu.au (H. Zhu).

0926-3373/$ – see front matter © 2007 Elsevier B.V. All rights reserved.
doi:10.1016/j.apcatb.2007.09.042

derivatives on a catalyst of about 1 wt.% gold dispersed on iron oxide (Au/Fe_2O_3 catalyst), and this catalyst was active for HCHO oxidation to CO_2 and H_2O at about 100 °C [11]. Although gold is a noble metal, its resource is more abundant compared with that of platinum, and thus its price is much lower than the price of platinum. Therefore, gold catalysts have great potential for removing volatile organic compound (VOC) gases from air [12–14]. Catalytic oxidation of formaldehyde on various catalysts, such as Pt/TiO_2 catalyst [15] and Ag/MnO_x-CeO_2 catalyst [16], has been reported, and recently there also are a few studies on gold catalysts loaded on various oxides for this reaction [11,17–19].

Ceria (CeO_2) is an essential component in the automobile three-way catalysts for its role in oxygen storage. CeO_2 can take up oxygen under oxidizing conditions and release it under reducing ones [20]. When ceria is used as a support for combustion catalysts, it absorbs and stores oxygen. As VOC species are adsorbed on a catalytic active component supported on ceria, such as gold, oxidizing the VOC species could be facilitated via reaction between the adsorbed species. Actually, the catalysts of gold supported on ceria (Au/CeO_2) are good combustion catalysts for many VOC substances, such as 2-propanol, methanol and toluene [14]. The oxidation of *n*-hexane and benzene over these catalysts were also investigated [13,21]. Recently, Deng et al. reported that gold-ceria catalysts with a low gold content exhibit good catalytic properties for the water–gas shift and preferential CO oxidation reaction. They found that after prolonged reaction at 120 °C, most of gold cations remained in ionic state [22]. Similar to other catalysts, the structure of the catalysts, in terms of crystallinity, dispersion and oxidation state of catalytic active component, as well as support structure and the interaction between active component and support, can be regulated by preparation approaches; and these structural factors are determinants on catalyst performance. Generally, the Au/CeO_2 or $Au/CeO_2/Al_2O_3$ catalysts were prepared by deposition–precipitation or co-precipitation, followed by calcinations at 400 or 500 °C [22–24]. Calcinations at these or higher temperatures convert gold species into metallic gold crystals with a size of 3–10 nm. Gold is the active component of these catalysts, so that its size, crystallinity and dispersion should significantly affect the catalyst performance. However, the relation between the gold crystal structure and the performance of Au/CeO_2 catalysts in literatures remains to be elucidated [25]. Such information will certainly be useful for understanding the reaction mechanism and design of efficient oxidation catalysts for effective removal of VOCs in indoor air.

The primary aim of the present research is, therefore, to acquire such information by studying the catalysts of gold supported on CeO_2, in which gold exists differently in terms of crystal structure. We prepared the catalysts by co-precipitation, with a much lower gold content, compared with that of the gold catalysts reported in literatures [13,14,23]. A calcination temperature of 300 °C was used, which is substantially lower than those reported in literatures, but yielding Au/CeO_2 catalysts with superior activity for HCHO oxidation although gold possesses a poor crystallinity in them. These catalysts are further heated at 400 °C or 700 °C, and the structure of the catalysts and the activity of the catalysts are examined.

2. Experimental

2.1. Preparation

A series of catalysts Au/CeO_2 were prepared by co-precipitation and calcined at 300 °C for 2 h. A 0.05 M solution of cerium nitrate was prepared with cerium nitrate hydrate ($Ce(NO_3)_3{\cdot}6H_2O$, AR grade, from Qi-Tong Rare Earth Co. Ltd., China) and deionized water. The solution with 2.43 mmol/L $HAuCl_4$ was prepared using $HAuCl_4$ (AR grade, from Beijing Chemical Reagent Co. Ltd., China) and deionized water. The 2.43 mmol/L $HAuCl_4$ solution was mixed with the 0.05 M $Ce(NO_3)_3$ solution. A 0.5 M solution of Na_2CO_3 was added dropwise into the mixture of $Ce(NO_3)_3$ and $HAuCl_4$ under vigorously stirring until the pH-value of the suspension reached 9 to precipitate cerium ions and gold ions simultaneously. The precipitate was then recovered and washed with warm deionized water until it was free of Cl^- ions according to a test with $AgNO_3$. Next, the wet cake obtained was dried in air at 80 °C and calcined at 300 °C for 2 h. Six samples with different gold contents were prepared by varying the ratio of the 2.43 mmol/L $HAuCl_4$ solution to the 0.05 M $Ce(NO_3)_3$ solution. They were named according to the gold content in the samples. Two more samples were obtained by calcination at 400 °C and 700 °C for 2 h, respectively, instead of the calcination at 300 °C. The sample name, gold content of the samples and the temperature at which the samples were calcined are given in Table 1.

2.2. Catalytic activity test

The catalytic activity test was conducted in a continuous-flow fixed-bed reactor of glass tube. The inner diameter of the tube was 0.8 cm, and 200 mg of the sample (40–60 mesh) was loaded into the reactor. The feed gas was 0.06 vol.% formaldehyde balanced with the air, which was obtained by passing an air flow through a solution of 36 wt.% HCHO at 0 °C. The space velocity of the experiment was 3.2×10^4 mL h^{-1}/g(catalyst). The effluent from the reactor was analyzed on-line using a Shimadzu DC-8A gas chromatograph equipped with a GDX 403 packed column and TCD detector. Chromatograph work station made by Zhejiang

Table 1
Gold content and calcinations conditions of the samples

Sample name	Au content (%)	Calcined temperature
0Au	0	300 °C (2 h)
0.26Au	0.26	300 °C (2 h)
0.34Au	0.34	300 °C (2 h)
0.70Au	0.70	300 °C (2 h)
0.78Au	0.78	300 °C (2 h)
0.85Au	0.85	300 °C (2 h)
0.78Au(400)	0.78	400 °C (2 h)
0.78Au(700)	0.78	700 °C (2 h)

University (China) was used to record and analyze the experiment data, by which HCHO, CO_2, H_2O, CO and HCOOH could be detected. Another approach for measuring the activity of the catalyst for the oxidation of HCHO was to conduct the experiments in a continuous-flow-bed reactor equipped with a CO_2-IR gas detector (type FQ-W-CO_2 made in Foshan, China). The concentration of CO_2 in effluent was recorded by CO_2-IR gas detector. This method was used in the case of complete oxidation of formaldehyde, and the conversion of HCHO can be expressed as $C_{CO_2}/C^*_{CO_2}$, where $C^*_{CO_2}$ is the concentration of CO_2 in the effluent when HCHO is oxidized completely and C_{CO_2} is that at different temperatures.

2.3. Characterization of the catalyst

X-ray powder diffraction (XRD) analysis of the samples was performed on a BRUKER D8 Advance diffract meter. Cu Kα radiation and 40 kV, 20 mA were used. Transmission electron microscopy (TEM) images were taken on JEM-2010 (Japan) to observe the particle morphology of the sample. Energy dispersed spectroscopy (EDS), which was used to determine elemental composition in a selected area of the specimen, was conducted on the same TEM. Gold content of the samples was measured by atomic absorption spectroscopy (AAS) technique using an Analyst 200 (P.E Co., U.S.A.). Thermal analysis was conducted on a Shimadzu DTG 50 instrument, from the ambient temperature to 800 °C. X-ray photoelectron spectroscopy (XPS) analysis was conducted on VG ESCALAB 210 spectrometer with Mg Kα irradiation, CAE = 30 eV and STEP = 60 meV to determine the binding energy of the Au4*f* electrons.

3. Results and discussion

The activity of the catalysts calcined at 300 °C is plotted against the gold content of the catalysts in Fig. 1. The activity was determined at a space velocity of 32,000 mL h^{-1}/g (catalyst). Compared to the support CeO_2 support, the catalysts of gold supported on ceria (Au/CeO_2) exhibit superior activity.

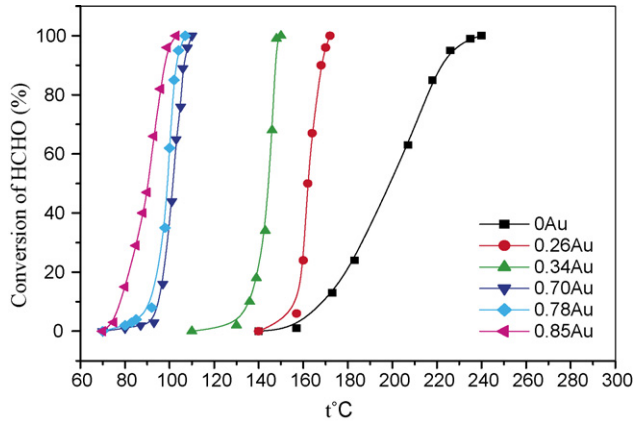

Fig. 1. Comparison of catalytic activity of the catalysts with different gold contents. All of catalysts were calcined at 300 °C for 2 h. The experimental conditions were: SV = 32000 h^{-1} mL/g cat, feed gas was 0.06 vol.% HCHO in air.

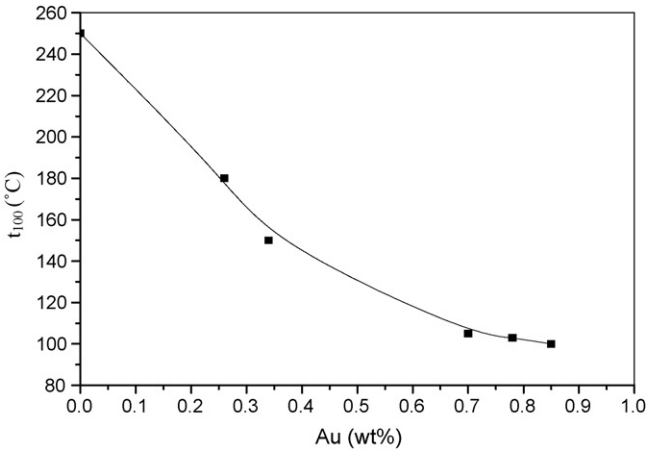

Fig. 2. The relationship between the temperature t_{100} (°C) and gold content in various catalysts which were calcined at 300 °C.

The catalytic activity increases with the gold content up to the largest gold content of this study, 0.85 wt.%. The 0.85Au sample exhibits the highest activity (Fig. 1 or Fig. 2). The catalyst with a gold content as low as 0.26 wt.% is much more active than the support ceria. Complete oxidation (100% HCHO conversion) is achieved on this catalyst at slightly above 160 °C, while the HCHO conversion over the support at 160 °C is merely about 10% and the complete oxidation was achieved at 250 °C. Fig. 1 also shows that elevating reaction temperature always increases HCHO oxidation rate, and the rate increases on the samples containing gold are much steeper than that on the ceria support.

The temperature at which HCHO is completely oxidized to CO_2 and water is denoted t_{100}. t_{100} can be used as an indicator of catalytic activity. The gold content of a catalyst is plotted against its t_{100} in Fig. 2.

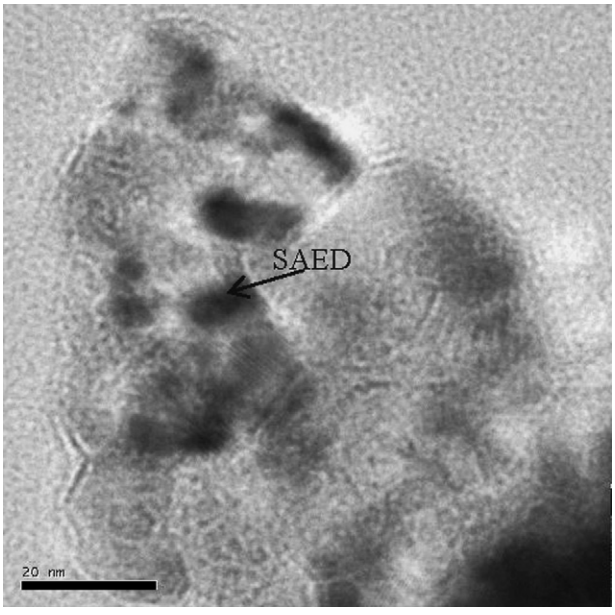

Fig. 3. TEM image of the 0.78Au sample.

t_{100} is about 107 °C and 103 °C for 0.78Au and 0.85Au samples, respectively. In contrast, t_{100} is 250 °C for 0Au sample which is the pure support CeO_2 (gold content is 0%), and a poor catalyst for the oxidation. The results in Figs. 1 and 2 confirm that gold is the catalytically active component for HCHO oxidation, in particular at low temperatures.

The sample of 0.78Au was investigated in details, as a representative, by TEM technique to understand the structure of the catalysts prepared by co-precipitation method. The TEM image of the 0.78Au sample is shown in Fig. 3. EDS results indicate the presence of gold in the dark area in Fig. 3. Gold is well dispersed on the surface of ceria and the Debye diffraction rings (Fig. 4) are observed in the selected area electron diffraction (SAED), suggesting that the dark areas in Fig. 3 are composed of small gold crystallites. This is different from the nanogold catalysts prepared by deposition–precipitation or co-precipitation and subsequent calcination at 400–500 °C, in which gold particles of about 3–5 nm were generally observed [26,27].

Thermal analysis result of 0.78Au sample calcined at 300 °C is provided in Fig. 5. The DTA curve indicates there is an endothermic reaction at 345.6 °C, which is accompanied by a 3.80% weight loss starting from 345.6 °C, according to the TG curve in the figure. This endothermic reaction is assigned to releasing of CO_2 from the sample. The weight-loss at temperatures below 345.6 °C is probably due to loss of water (5.40%). The overall weight loss is 9.20%. The calcination at 300 °C could not completely remove carbonate in the 0.78Au sample. Carbonate in the sample cannot affect the measurement of the catalytic activity because the temperature of the activity test is far below 345.6 °C, the decomposing temperature of carbonate. The effect of carbonaceous species on the activity of catalysts has not been observed in this study.

The high resolution TEM image of the 0.78Au sample was taken and is illustrated in Fig. 6. The fringes of the CeO_2 crystal lattice are clear. The distance between two adjacent lattice

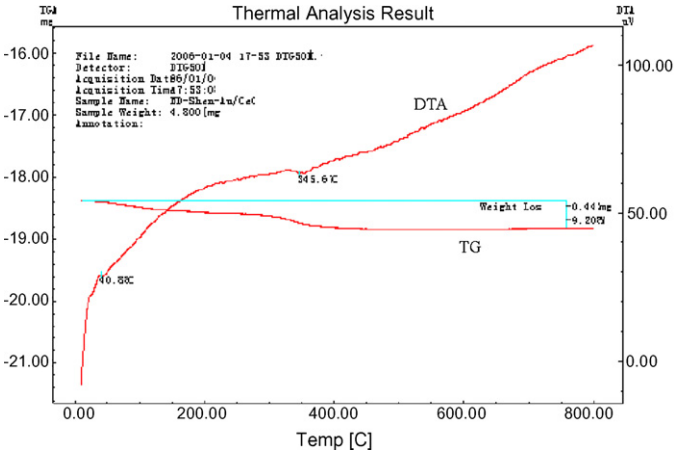

Fig. 5. Thermal analysis result of the 0.78Au sample.

planes was measured to be 0.31 nm which is consistent with the d-value of the 1 1 1 lattice planes of CeO_2 (d = 0.316 nm). The sizes of CeO_2 crystals are between 30 and 50 nm. Nevertheless, we could not find gold crystals with the fringes of gold lattice even when the magnification was increased further. Gold readily form crystallites of about 3–5 nm in size when loaded onto support [24–27]. But the situation in the present study is distinctly different: gold exists as well-dispersed particles with a poor crystallinity.

The TEM image of 0.78Au(400) sample, which was obtained by calcining the 0.78Au sample further at 400 °C for 2 h, is shown in Fig. 7.

The calcination at 400 °C converted the gold crystallites into larger metallic gold crystals. As can been seen in Fig. 7, the size of gold crystals is not uniform. The largest particle size is about 20 nm, and the mean size of gold particles was about 10 nm

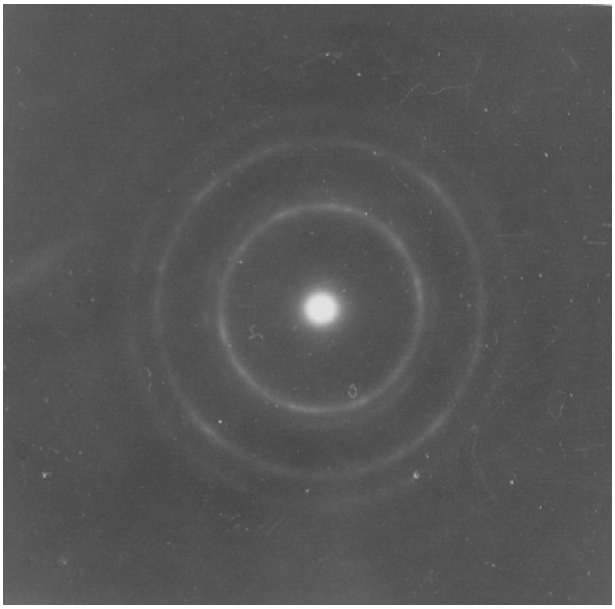

Fig. 4. SAED patterns of Au on 0.78Au sample. $L\lambda = 2.76$, $d_{111} = 2.35$, $d_{220} = 1.43$.

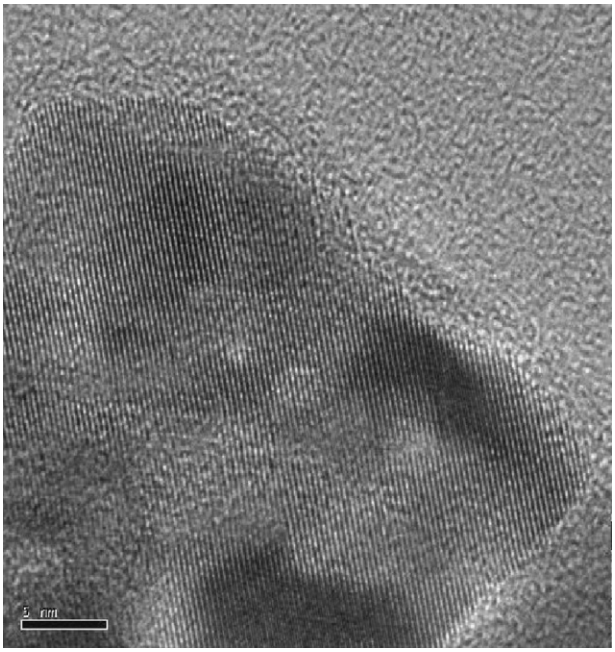

Fig. 6. High resolution TEM image of the 0.78Au sample. The fringes in the image are from CeO_2 lattice.

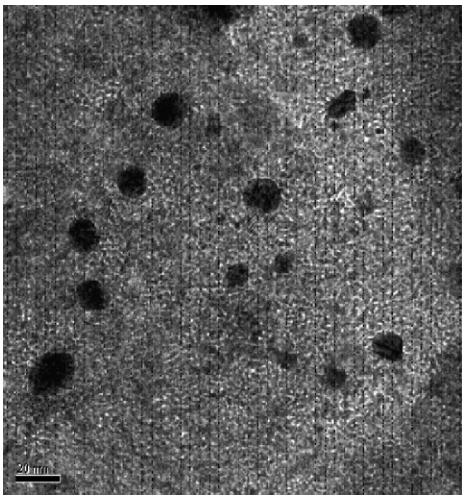

Fig. 7. TEM image of 0.78Au(400) sample. The dark particles are gold crystals.

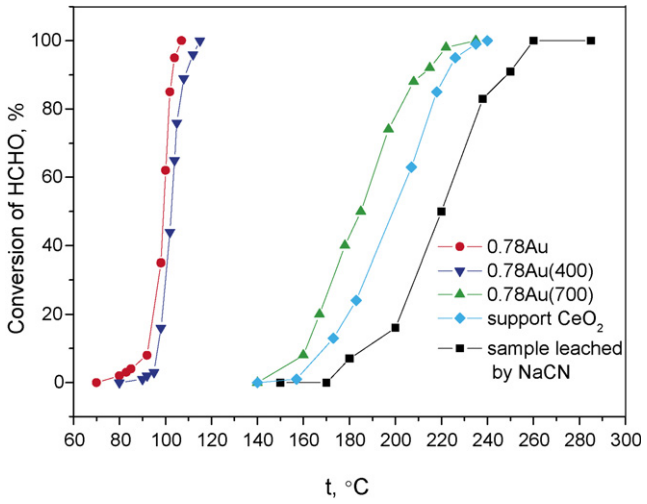

Fig. 9. The function of temperature on the activity of various catalysts as well as support ceria.

estimated from the image. It is also noted in Figs. 7 and 8 that the boundary between gold particles and support ceria is not distinctly clear. This is probably due to diffusion of CeO_2 over the surface of the gold crystals [28]. The interaction between gold and support is important, which can weaken the crystallinity of the gold particles and may enhance the catalytic activity for HCHO oxidation.

The activity of catalyst which was calcined at 400 °C is lower than that of the catalyst calcined at 300 °C (Fig. 9): t_{100} of the former is 115 °C and t_{100} of the latter is 107 °C.

The difference in activity can be related to the structures of the catalysts. Gold in a sample calcined at 300 °C for 2 h (for instance, 0.78Au in Fig. 3) exists in crystallites which is super active to the reaction. But, gold in the corresponding sample calcined at 400 °C for 2 h, 0.78Au(400), exists in crystals with a mean diameter of about 10 nm. Obviously, the smaller the size of particles, the better the activity for HCHO oxidation is.

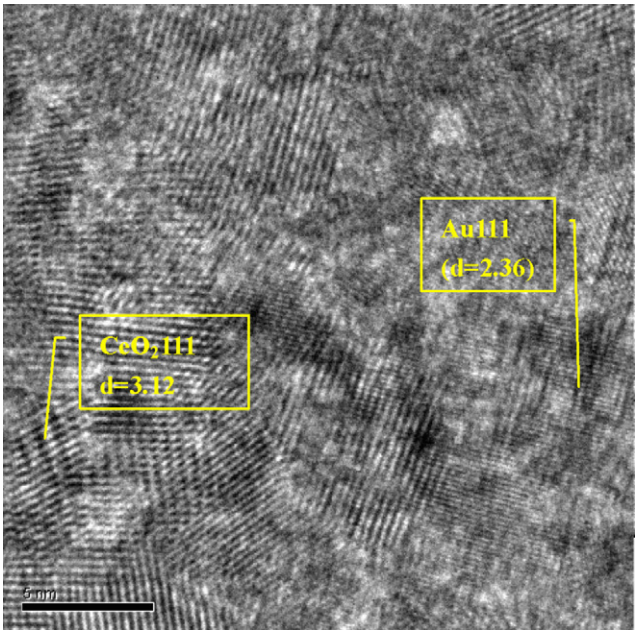

Fig. 8. High resolution TEM image of 0.78Au(400), the fringes in the image are from the CeO_2 lattice and Au lattice, respectively, as indicated.

Figs. 10 and 11 show the XPS spectra of several samples in the Au4*f* region. The peaks assigned to Au^0 could not be found in the spectrum of sample 0.78Au(65) which was sample 0.78Au dried at 65 °C without calcinations. It means that in this sample, gold exists in valence states such as Au^{3+} and Au^+. The XPS spectrum of sample 0.78Au apparently shows the existence of Au^{3+} and Au^0 in this sample. This indicates that part of the gold in valence states was reduced into metallic state during the calcination at 300 °C [29]. This result is in accordance with the TEM observation (Fig. 3) and the SAED (Fig. 4) result of this sample. Margilifalvi et al. denoted the mixed ensemble as $(Au^{\sigma+})_m$–$(Au^0)_n$ and proposed that the activation of CO was related to the formation of $(Au^{\sigma+})_m$–$(Au^0)_n$ [30] which might be similar to the oxidation of HCHO on the 0.78Au sample. The XPS spectrum of sample 0.78Au(400) shows a further reduction of the gold in high valence states into metallic or low valence states. Less Au^{3+} can be found in this sample. When the sample 0.78Au is calcined at

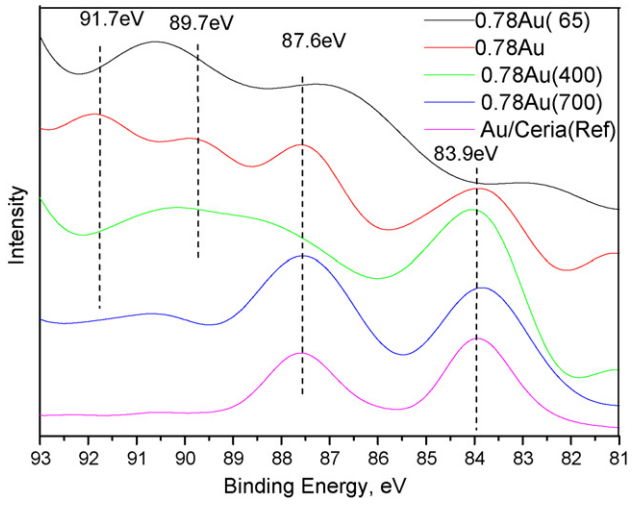

Fig. 10. XPS spectra of the samples.

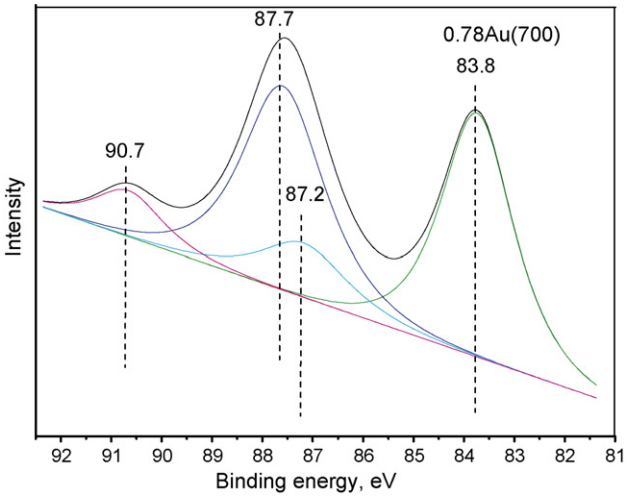

Fig. 11. XPS spectra of sample 0.78Au(700).

700 °C, most gold in the obtained sample 0.78Au(700) is in metallic state but small amount of gold is still in high valencies (Fig. 11). It seems that the valency of gold is between Au^{3+} and Au^{+}, which, actually, is caused by the substitution of Ce^{4+} by Au^{3+} in the ceria lattice. When the substitution process occurs, oxygen vacancies close to Au^{3+} are produced, which must result in the weakening of the positive potential around Au^{3+} and thus the negative shift of the peak position of Au^{3+} in the XPS spectrum. The spectrum of sample Au/ceria (Ref) which was prepared by $NaBH_4$ reduced gold colloid immobilized on ceria shows only Au^0 in this sample, indicating not only the calcinations temperature affects the gold state but the preparation method as well.

As anticipated, heating the 0.78Au sample at even higher temperatures results in larger gold crystals. After a calcination at 700 °C for 2 h, the size of gold particles in this sample increases to 40–50 nm (Fig. 12). Moreover, the perimeter of the interface between gold and ceria, which might be the active sites for the reaction [31], greatly decreases, and gold particles seem to connect with ceria support by touching and not by fusing. As a result, the interaction with the ceria support becomes less important.

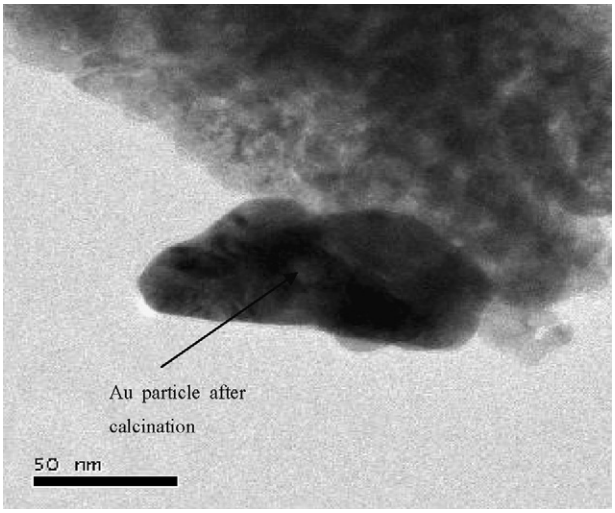

Fig. 12. TEM of the 0.78Au sample calcined further at 700 °C for 2 h.

By carefully comparing the XRD patterns we found an interesting structural feature of the 0.78Au(700) sample: the ceria lattice in this sample is smaller than those in the corresponding samples heated at lower temperatures. The positions of diffraction peaks from ceria in the sample 0.78Au and sample 0.78Au(400) are the same as those in the standard pattern of ceria, except that the widths of the peaks are slightly different because the particle size of ceria in 0.78Au is smaller than that in 0.78Au(400). But the diffraction peaks of ceria in 0.78Au(700) shift towards the direction of large 2θ, indicating a decrease in d values, and thus in the lattice parameters of ceria. The average lattice constant of 0.78Au(700) is 0.5372 nm, calculated from the positions of the 1 1 1, 2 0 0 and 2 2 0 diffractions of ceria (Fig. 13). The calculated value for 0.78Au(400) is 0.5400 nm, almost the same as the standard value $a = 0.5410$ nm [32]. At high temperatures (such as 700 °C) the mobility of ions increases. It is possible that Au^{3+} ions enter into lattice of ceria, occupying some sites that are normally occupied by Ce^{4+} ions in ceria. The effective ion radius of Au^{3+} ions is 0.085 nm which is smaller than that of Ce^{4+} ions, 0.087 nm [33]. Such a substitution could cause the lattice contraction. The Au^{3+} in sample 0.78Au(700), identified by XPS (Figs. 10 and 11), should exist in the lattice of ceria. Venezia et al. [34] reported that in Au/CeO_2 catalysts prepared by CP or DP method, $Ce_{1-x}Au_xO_{2-\delta}$, where δ denotes the charge balance, formed when the samples were heated, resulting in the shrinkage of ceria lattice, which could be detected by XRD.

The 0.78Au(700) sample was leached with an aqueous solution of 2 wt.% NaCN overnight. The lattice constant of the

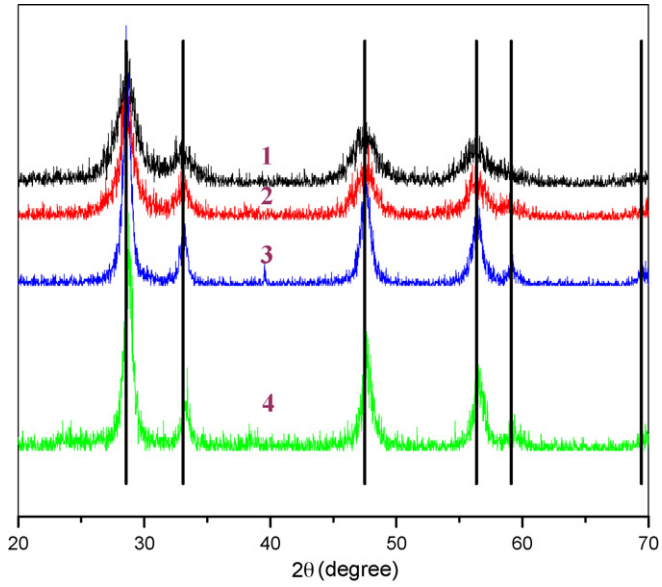

Fig. 13. XRD patterns of various Au/CeO_2 catalysts. From top to the bottom: 0.78Au sample (heated at 300 °C), 0.78Au(400) sample (heated at 400 °C), 0.78Au(700) sample leached by NaCN solution (2 wt.%), and 0.78Au(700) sample (heated at 700 °C). Vertical lines indicate the positions of the diffraction peaks of ceria.

leached sample is 0.5400 nm derived from its XRD pattern (pattern 3 in Fig. 13). The patterns and the parameter are almost as the same as those of the sample 0.78Au(400). As shown in Fig. 9, the activity of the leached 0.78Au(700) is even worse than that of ceria as the Au^{3+} ions are leached out. The facts that the sample calcined at 700 °C has a smaller surface area than the sample calcined at 400 °C, and the leaching inevitably causes change in the surface property may explain the poor activity of the leached sample. Fu et al. have reported catalysts of gold and cerium oxide with low gold content prepared by NaCN leaching method. They found increase in lattice parameters due to Ce^{3+} formation or due to Au^{3+}, or both [23]. However, in the present study, after the sample was leached by the NaCN solution, the lattice constant of ceria was restored, which should be attributed to the leaching out of Au^{3+} in the lattice of ceria or the reduction of a small part of Ce^{4+} into Ce^{3+} by NaCN.

4. Conclusion

In summary, Au/CeO_2 catalysts with low gold content ($\leq$0.85 wt% in this study) and calcined at 300 °C have superior catalytic activity for HCHO oxidation at temperature about 100 °C. In the studied range of gold content, the catalytic activity for HCHO oxidation increases with the increasing gold content. More importantly, the catalytic activity of the catalysts is closely related to the crystal structure of gold in the catalysts. The highly dispersed and poorly crystallized metallic gold and small amount of oxidized gold in the catalysts exhibits superior catalytic activity for HCHO oxidation. Further heating the catalyst at 400 °C results in not only the formation of well crystallized gold nanocrystals, but also obvious decrease in catalytic activity. Therefore, manipulating the synthesis parameters to achieve highly dispersed gold species is crucial for developing efficient gold catalyst for HCHO oxidation. The calcination at 700 °C yields large gold crystals which has poor catalytic activity, but at the same time it promotes the substitution of Ce^{4+} ions by Au^{3+} ions in the ceria lattice causing lattice contraction as shown XRD and XPS results. Leaching the 0.78Au(700) sample with NaCN solution removes the Au^{3+} ions, restoring in the standard lattice constant of ceria. But, the activity of the leached sample is even worse than that of ceria. In addition to a new synthesis approach for Au/CeO_2 catalysts, this study also provides useful knowledge of the structure of related catalysts. The finding that the Au^{3+} ions could be stabilized in the lattice of ceria at 700 °C is important for understanding the properties of supported gold catalysts.

Acknowledgements

Financial support for this work came from the National Science Foundation of China (20263001, 20563003) and from the Australian Research Council (ARC).

References

[1] International Agency for Research on Cancer, IARC Monographs on the Evaluation of the Carcinogenic Risk of Chemicals to Humans, Some Industrial Chemicals and Dyestuffs, Lyon, France, vol. 29, 1982, p. 416.
[2] Agency for Toxic Substances and Disease Registry, Public Health Service, U.S. Department of Health and Human Services, Toxicological Profile for Formaldehyde, NTIS Accession No. PB99-166654, 1999, p. 451.
[3] National criteria of the People's Republic of China, criterion for controlling the indoor air pollutant in civil architecture projects, GB50325-2001.
[4] X.Z. Yang, Y.N. Shen, Z.F. Yuan, H.Y. Zhu, J. Mol. Catal. A. 237 (2005) 224–231.
[5] A. Hinz, M. Skoglungh, E. Fridell, A. Andersson, J. Catal. 201 (2001) 247–257.
[6] C. Lahousse, A. Bernier, P. Grange, B. Delmon, P. Papaefthimiou, T. Ioannides, X. Verykios, J. Catal. 178 (1998) 214–225.
[7] R. Spinici, M. Faticanti, P. Marini, S. De Rossi, P. Porta, J. Mol. Catal. A. 197 (2003) 147–155.
[8] Y.H. Sun, Y.N. Shen, M.L. Jia, R.S. Hu, Acta Physico-Chim. Sin. 15 (1999) 720.
[9] M. Haruta, S. Tsubota, T. Kobayashi, H. Kageyama, J. Catal. 144 (1993) 175–192.
[10] M. Haruta, N. Yamada, T. Kobayashi, S. Iijima, J. Catal. 115 (1989) 301–309.
[11] M. Haruta, A. Ueda, S. Tsubota, R.M.T. Sanchez, Catal. Today 29 (1996) 443–447.
[12] S. Scire, S. Minico, C. Crisafulli, S. Galvagno, Catal. Commun. 2 (2001) 229–232.
[13] M.A. Centeno, M. Paulis, M. Montes, J.A. Odriozola, Appl. Catal. A. 234 (2003) 65–78.
[14] S. Scire, S. Minico, C. Crisafulli, S. Cristina, P. Alessandro, Appl. Catal. B. 40 (2003) 43–49.
[15] C. Zhang, H. He, K. Tanaka, Catal. Commun. 6 (2005) 211–214.
[16] X. Tang, J. Chen, Y. Li, Y. Li, Y. Xu, W. Shen, Chem. Eng. J. 118 (2006) 119–125.
[17] M. Jia, Y. Shen, C. Li, Z. Bao, S. Sheng, Catal. Lett. 99 (2005) 235–239.
[18] C. Li, Y. Shen, M. Jia, S. Sheng, M.O. Adebajo, H. Zhu, Catal. Commun. (2007) in press.
[19] Y. Shen, Patent of China, Zl200510067178.9 (2006).
[20] A. Trovarelli, Catal. Rev. Sci. Eng. 38 (1996) 439–520.
[21] S.Y. Lai, Y. Qiu, S. Wang, J. Catal. 237 (2006) 303–313.
[22] W. Deng, J.D. Jesus, H. Saltsburg, M. Flytzani-Stephanopoulos, Appl. Catal. A. 291 (2005) 126–135.
[23] Q. Fu, W. Deng, H. Saltsburg, M. Flytzani-Stephanopoulos, Appl. Catal. B 56 (2005) 57–68.
[24] M.A. Centeno, M. Paulis, M. Montes, J.A. Odriozola, Appl. Catal. A. 234 (2002) 65–78.
[25] N. Weiher, E. Bus, L. Delannoy, C. Louis, D.E. Ramaker, J.T. Miller, J.A.V. Bokhoven, J. Catal. 240 (2006) 100–107.
[26] H.H. Kung, M.C. Kung, C.K. Costello, J. Catal. 216 (2003) 425–432.
[27] N. Lopez, T.V.W. Janssens, B.S. Clausen, Y. Xu, M. Mavrikakis, T. Bligaard, J.K. Nørskov, J. Catal. 223 (2004) 232–235.
[28] P.X. Huang, F. Wu, B.L. Zhu, X.P. Gao, H.Y. Zhu, T.Y. Yan, W.P. Huang, S.H. Wu, D.Y. Song, J. Phys. Chem. B 109 (2005) 19169–19174.
[29] Q. Fu, S. Kudriavtseva, H. Saltsburg, M. F-Stephanopoulos, Chem. Eng. J. 93 (2003) 41–53.
[30] J.L. Margitfalvi, A. Fasi, M. Hegedus, F. Lonyi, S. Gobolos, N. Bogdanchikova, Catal. Today 72 (2002) 157–169.
[31] M. Haruta, Gold Bull. 37 (2004) 27–36.
[32] X-ray powder diffraction file carried by BRUKER D8 ADVANCE.
[33] R.D. Shannon, Acta Cryst. A 32 (1976) 751–767.
[34] A.M. Venezia, G. Pantaleo, A. Longo, G.D. Carlo, M.P. Casaletto, F.L. Liotta, G. Deganello, J. Phys. Chem. B 109 (2005) 2821–2827.